PHYSICAL REVIEW B VOLUME 15, NUMBER 10 15 MAY 1977

Electronic-energy-structure calculations of silicon and silicon dioxide using the extended tight-binding method

S. Ciraci* and I. P. Batra
IBM Research Laboratory, San Jose, California 95193
(Received 23 August 1976)

We have studied the electronic energy structure of silicon and silicon dioxide using the extended tight-binding method. For silicon, we found that the basis set in terms of single Gaussian-type orbitals is able to reproduce the band structure which is in good agreement with the experimental data. However, simple linear combination of atomic orbitals failed to describe the band order of the lower conduction bands. For silicon dioxide, we calculated the energy band, total and orbital densities of states of β-cristobalite. In terms of these, we obtained a consistent interpretation of various experimental measurements on amorphous silicon dioxide. Furthermore, by examining the orbital character and the calculated charge densities of various states, we determined the origin of the bonding in silicon dioxide.

I. INTRODUCTION

The paper presents our results for the electronic structure of silicon and β-cristobalite (ordered SiO_2) using the extended tight-binding (ETB) method.[1-4] Even though silicon is one of the most studied materials by solid-state physicists, there are several reasons for us starting with the band-structure calculation of silicon. Although previous energy-band models have been successful in interpreting experimental data, there have been serious discrepancies at some crucial points. One such discrepancy has been the ordering of the lower conduction bands at the center of the Brillouin zone. The linear combination of atomic orbitals (LCAO) calculation of Chaney *et al.*[5] (which is practically similar to the present one) and the self-consistent orthogonalized-plane-wave (OPW) calculation of Stukel and Euwema[6] predicted the reverse order for $\Gamma_{2'}$ and Γ_{15}, although it is well accepted that $\Gamma_{2'}$ lies above Γ_{15}.[7-9] To gain confidence in our method for further studies of oxides of Si, we calculate the band structure of Si and try to understand why a previous LCAO calculation failed to obtain the proper band ordering. Consequently, this work represents an effort to resolve the discrepancy between the LCAO[5] and the other band-structure calculations.[8,9] Furthermore, a converged basis set which is able to accurately represent the electronic structure of silicon can be used in the study of the oxides of silicon.

For the oxides of silicon, which are the essential ingredients in metal-oxide-semiconductor devices, there is little known theoretically. In this paper, we have also studied the electronic structure of β-cristobalite (which is a highly ordered form of SiO_2) as a next step in understanding the oxides of silicon. Silicon dioxide has been investigated using photoemission and other optical experiments.[10-19] Recently, extensive interest in the electronic properties of the clean and adatom-adsorbed silicon surfaces has brought SiO_2 into focus. For the identification of the surface states, Wagner and Spicer[18] measured the photoemission from the oxygen-adsorbed cleaved silicon surface. They observed spectra quite similar to the ultraviolet photoemission spectra (UPS) obtained from amorphous SiO_2.[16] Lately, Auger electron spectroscopy, ellipsometry, and electron spectroscopy of surface vibrations by Ibach *et al.*[19] and electron-energy-loss spectra by Ibach and Rowe[17] clearly revealed differences between the oxidation state of silicon and the oxygen adsorption on silicon surface. In the former, the spectra have been found to be quite similar to the spectrum of amorphous SiO_2. On the other hand, photoemission spectra from the oxygen-adsorbed silicon surface does not show any similarity to the UPS spectra of amorphous SiO_2. From this point of view, we believe that the spectral analysis of SiO_2 is important for an understanding of the oxidation of Si. Apart from the interest in the oxygen adsorption on silicon surfaces, the study of the electronic structure of β-cristobalite is important for the following reasons. The similarity of the reflectivity spectra of amorphous SiO_2 and α-quartz[10] indicates that the overall features of the valence-band distribution for various allotropic forms of SiO_2 should be quite similar. Therefore, one expects that our calculated state distribution should be comparable to the ultraviolet and x-ray photoemission (UPS and XPS) spectra for amorphous SiO_2.[16] Any deviations might be attributed to the amorphousness of the experimental samples. While some of the information we report is specific to β-cristobalite, many of our conclusions concerning the state distribution, bonding, etc., are likely to be of general applicability to other

allotropic forms of SiO_2.

Previously Bennett and Roth[20] and Yip and Fowler[21] carried out the cluster model calculations for the energy-level structure of SiO_2. Recently, Pantelides and Harrison[22] carried out empirical calculations for crystalline SiO_2 based on the bond-orbital model,[23] where the bond orbitals of SiO_2 were constructed from silicon sp^3 hybrid and oxygen atomic orbitals. A similar basis set was also previously used by Reilly.[24] Work by Schneider and Fowler[25] reported first detailed band-structure calculations where the basis set consisting of nonoverlapping atomlike functions and plane waves were used. Our work is carried out from first principles without any *a priori* knowledge of either the energy bands or the experimentally determined spectrum. We set up a one-electron Hamiltonian using the crystal potential constructed by a superposition of atomic potentials and employ the Kohn-Sham exchange parameter ($\alpha = \frac{2}{3}$). The resulting equation is then solved using an appropriate atomic basis set without introducing any adjustable parameters.

The remainder of this paper is organized as follows: In Sec. II, the major steps of the ETB method are discussed. In Sec. III, we discuss the electronic band-structure of silicon calculated by the present method. In particular, we show that the Bloch sums based on the single Gaussian-type orbitals (GTO), rather than the atomic orbitals (AO), are more appropriate for describing the energy states of silicon. Also, we show that the basis set consisting of the sp^3 hybrid orbitals is nearly as bad as the atomic orbitals in representing the conduction band. The results for β-cristobalite are presented in Sec. IV. The energy-band structure, total and orbital densities of states, and charge density are discussed and compared with the available experimental data and with previous theoretical works. In particular, our results using the AO basis set agree with the band structure calculated by Schneider and Fowler.[25] In Sec. V, a new parametrization scheme is suggested, which may be useful for the investigation of solids containing many atoms per unit cell. This scheme is put in perspective by examining the extended Hückel method at the same time. Finally, in the last section main results are summarized. The electronic properties of the oxygen adsorbed on the Si(111) surface and silicon-SiO_2 interface will be the subject of a future publication.

II. EXTENDED TIGHT-BINDING METHOD

The tight-binding method[26] is one of the earliest models in the energy band theory. The earlier applications of the tight-binding method had not been successful because of the immense difficulties in the evaluation of the multicenter integrals. Therefore, the empirical version of the method has been preferably used as an interpolation scheme for the energy-band structure, where the matrix elements have been determined from experiments or other band calculations.[27] Not long ago, Lafon and Lin[1] showed that the tight-binding method can be used as a first-principles method if the multicenter integrals are properly calculated. By now, the method has been applied to a wide range of bulk related problems.[1-3] Recently, Ciraci and Batra[4] for the first time used the method self-consistently in studying the surface electronic structure of diamond. It should be noted that the name "tight-binding" method has been used in the literature for calculations performed at various levels of sophistications (from the simple empirical version to the calculations including self-consistency). Our purpose in adding the word "extended" in front of the "tight binding" is to indicate the level of sophistication implied in the present work.

In the ETB method one expresses the wave function as a linear combination of the Bloch sums,

$$X_i(\vec{k},\vec{r}) = [N\Omega_i(\vec{k})]^{-1/2} \sum_l e^{i\vec{k}\cdot(\vec{R}_l+\vec{\tau}_i)} \psi_i(\vec{r}-\vec{R}_l-\vec{\tau}_i). \tag{1}$$

Here $\vec{R}_l$ and $\vec{\tau}_i$ denote the primitive and nonprimitive translation vectors. $\Omega_i(\vec{k})$ is the factor which normalized the Bloch sums $X_i(\vec{k},\vec{r})$. $\psi_i(\vec{r})$ stands for the Gaussian-type orbitals (or the atomic orbitals as in the LCAO method). In our calculations, the crystal potential was constructed by overlapping atomic potentials[28] which were "nearly self-consistent" for tetrahedrally coordinated semiconductors.[8] In the ETB method, the crystal potential is treated similar to the Ewald procedure where the slow convergent core potential $V_c(\vec{r})$ is expressed in terms of Gaussians centered at each atomic site.[29]

$$V_c(\vec{r}) = \sum_{l,i} \left(\frac{-2Z_i - \alpha_i}{r_{li}} e^{-\beta_{1i} r_{li}^2} + \frac{\alpha_i}{r_{li}} e^{-\beta_{2i} r_{li}^2} + \sum_{t=3}^{m} \eta_t e^{-\beta_{ti} r_{li}^2} \right), \tag{2}$$

where $r_{li} = |\vec{r} - \vec{R}_l - \vec{\tau}_i|$, and Z is the nuclear charge. The coefficients α, η, and the exponents β in Eq. (2) are carefully chosen such that the remaining smooth potential $V_s(\vec{r})$, including the local exchange potential, can be expanded in a rapidly convergent Fourier series, i.e.,

$$V_s(\vec{r}) = \sum_{\vec{G}} V_s(\vec{G}) e^{-i\vec{G}\cdot\vec{r}}. \tag{3}$$

Here $\vec{G}$ denotes the reciprocal-lattice vectors.

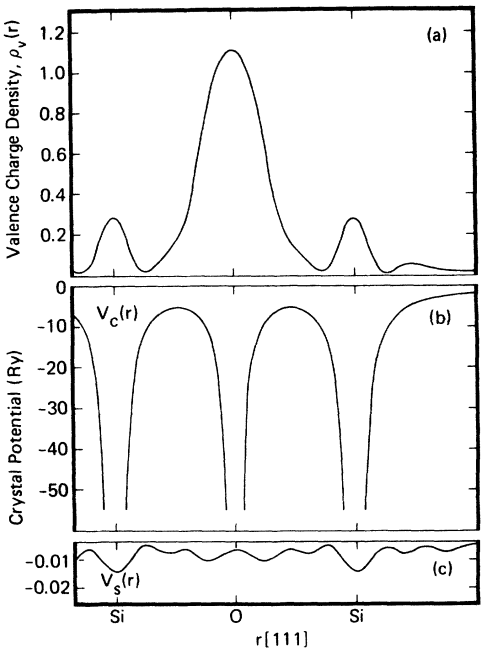

FIG. 1. (a) Valence charge density of β-cristobalite along the Si-O-Si chain (unit is electron/unit cell). (b) The core potential $V_c(\vec{r})$ for β-cristobalite. (c) The smooth potential $V_s(\vec{r})$.

Note that such a decomposition of the total potential into core and smooth potential is only a computational convenience. The final potential $V_s(\vec{r}) + V_c(\vec{r})$ is independent of the constants in Eq. (2). Figure 1 illustrates the core and smooth components of the SiO_2 total potential treated in mixed space. One can easily observe the smoothness of $V_s(\vec{r})$ by comparing the energy scale in Figs. 1(b) and 1(c). In Table I, the coefficients and exponents used in describing the core potential are listed.

To form the secular equation $[H(\vec{k}) - E(\vec{k})S(\vec{k})]a(\vec{k}) = 0$ the overlap matrix elements and the matrix elements of the smooth potential are calculated from the generalized overlap matrix[3]

$$W_{ij}(\vec{G},\vec{k}) = [\Omega_i(\vec{k})\cdot\Omega_j(\vec{k})]^{-1/2} \times \sum_l e^{i\vec{k}\cdot(\vec{R}_l+\vec{\tau}_j-\vec{\tau}_i)} \langle \psi_i(\vec{r}-\vec{\tau}_i)| e^{i\vec{G}\cdot\vec{r}} \times |\psi_j(\vec{r}-\vec{R}_l-\vec{\tau}_j)\rangle. \quad (4)$$

The matrix elements of W, kinetic energy, and the core potential are calculated analytically.

For a better understanding of the present method, it may be useful to compare it with a method which uses a nearly-free-electron model. For this purpose the OPW method[30] may be most convenient because both methods (ETB and OPW) determine the band structure from variational principles and there is a close relationship between them, as established by Parmenter.[29] A major difference, however, lies in the choice of "basis set." In OPW, the basis set is expressed in the mixed space, whereas the crystal potential is treated completely in the reciprocal space. In the ETB method (as used in the present study), the basis set is expressed completely in the direct space, whereas the crystal potential is treated in the mixed space. The size of the secular matrix in the OPW method determines to what extent the crystal potential, and consequently the basis set in the reciprocal space, is sampled. The convergence problem may arise if the size of the unit cell is large. In the ETB method, the basis set and the crystal potential are independent of each other. By treating the core potential in the direct space, one can achieve a high degree of accuracy in calculating the matrix elements of highly localized GTO's. In both OPW and ETB methods, valence-state wave functions are practically similar at the core region. This is achieved in OPW by orthogonalizing the plane waves to the core states. In the ETB method, the variational principle determines the wave function in the core

TABLE I. Coefficients and exponents representing the core potential of silicon and oxygen atoms.

Silicon		Oxygen	
$-2Z-\alpha = -1.78$	$\beta_1 = 4538.08$	$-2Z-\alpha = -1.15$	$\beta_1 = 4057.24$
$\alpha = -26.22$	$\beta_2 = 90.38$	$\alpha = -14.85$	$\beta_2 = 95.54$
$\eta_3 = -17.41$	$\beta_3 = 2.69$	$\eta_3 = -15.35$	$\beta_3 = 4.57$
$\eta_4 = -2.13$	$\beta_4 = 0.27$	$\eta_4 = -2.20$	$\beta_4 = 0.60$
$\eta_5 = -4.92$	$\beta_5 = 0.79$	$\eta_5 = -7.56$	$\beta_5 = 1.68$
$\eta_6 = -47.24$	$\beta_6 = 9.63$	$\eta_6 = -29.64$	$\beta_6 = 13.38$
$\eta_7 = 128.18$	$\beta_7 = 153.60$	$\eta_7 = 70.16$	$\beta_7 = 154.06$
$\eta_8 = -92.07$	$\beta_8 = 31.14$	$\eta_8 = -52.45$	$\beta_8 = 36.51$
$\eta_9 = -0.53$	$\beta_9 = 0.07$	$\eta_9 = -0.72$	$\beta_9 = 0.18$
$\eta_{10} = -0.16$	$\beta_{10} = 0.03$	$\eta_{10} = -0.16$	$\beta_{10} = 0.07$

region. Outside the core region, the limited number of plane waves are left to describe the wave function in OPW. The limited number of OPW's have been proven to describe adequately the wave functions of metals and covalent semiconductors. However, a convergent description of a wave function of highly ionic solids, or solids for which there is no core state to orthogonalize to, may require a large number of OPW's.[31] As a matter of fact, the solution of the transition metals by OPW represents an immense difficulty, although this difficulty can be overcome by considering d states as a core, and by appropriately calculating their overlap integrals. In the ETB method, the wave functions outside the core are described by a limited number of GTO's. Although this has the advantage because one is dealing with a small size secular matrix, sometimes small basis set may not appropriately describe the conduction-band wave functions outside the core region. Certainly, the GTO basis set is[3] superior to the AO basis set in describing the conduction band states where the atomic origin may be lost. To overcome this difficulty one uses GTO's corresponding to excited states. Even the GTO's can be placed at the interatomic sites for a better description of the wave function (such as the bond charge in covalent solids).[32] On the other hand, the basis set may have one or more GTO's with very small exponents, whose overlaps should be calculated up to many distant neighbors to avoid spurious linear dependency or the overlap catastrophe.[33] Since the diffused GTO's can be easily expanded in the momentum space, the above difficulty can also be circumvented in mixed space, as suggested by Parmenter.[29] At this point, one can even follow a different route, where the basis set consisting of GTO's and single plane waves, or plane waves orthogonalized to GTO's, are used. Mixed basis set has been used by Ciraci[34] by treating the plane-wave part as a perturbation. He showed that the addition of plane waves can further improve the band structure obtained from LCAO calculations. Hopefully, this extension, by using additional basis set in the ETB method, brings us to a point where the disadvantages of both methods are minimized.

As to the computational aspects of the plane waves used with the GTO's, the matrix elements coupling two plane waves are easily calculated. The matrix elements between a plane wave and a GTO can be expressed as follows:

$$\langle X_i(\vec{k},\vec{r})|H|\vec{k}+\vec{G}\rangle = |\vec{k}+\vec{G}|^2 X_i(\vec{k}+\vec{G}) + \sum_{\vec{G}''} V_s(\vec{G}'')X_i(\vec{k}+\vec{G}-\vec{G}'') + \langle X_i(\vec{k},\vec{r})|V_c(\vec{r})|\vec{k}+\vec{G}\rangle. \quad (5)$$

Here

$$X_i(\vec{k}+\vec{G}) = [\Omega_i(\vec{k})U]^{1/2} e^{i\vec{G}\cdot\vec{\tau}_i}\psi_i(\vec{k}+\vec{G}). \quad (6)$$

This is the Fourier component of the Bloch sum $X_i(\vec{r})$. In Eq. (5) the third term on the right-hand side, i.e., the matrix elements of the core potential can be calculated analytically by using multiplication properties of two Gaussians. In the present calculation, the basis set for Si and O does not contain very diffused Gaussians. Therefore, the augmentation of the basis set by plane is not necessary.

We finish this section with a few final remarks about the ETB method. Since the basis set consists of s, p, and d type of GTO's, the ETB method offers a conceptual simplicity in understanding the nature of the bands and bonds. As a computational advantage in the ETB method, the wave vector-$\vec{k}$ dependency can be extracted from the Bloch states and then the overlap integrals over the orbital part are calculated once for all.

III. ENERGY BAND STRUCTURE OF SILICON

As mentioned earlier, the ordering of the conduction bands of silicon has been subject of some controversy. Recently, low-field electroreflectance measurements of Aspnes and Studna[7] and pseudopotential calculations of Chelikowsky and Cohen[9] proved that the $\Gamma_{2'}$ lies above Γ_{15}, contrary to the previous LCAO calculations.[5] To reexamine the electronic structure of silicon, we start with the Bloch sums constructed from single[3] GTO's, rather than AO's. In this way, the coefficients of the GTO's have full variational freedom. Thus, wave functions of Si are expressed as a linear combination of 70 s-, p-, and d-type GTO's.[35] The interactions between GTO's up to 20 a.u. apart are included. The core potential [as defined in Eq. (2)] is expanded in terms of 10 s- and p-type Gaussians, each centered at the atomic sites (see Table I). The remaining part, which was called the smooth potential, is expanded in the reciprocal space to convergence. Note that by using a larger number of Gaussians in Eq. (2), one may treat the total crystal potential in the direct space. However, the higher the number of Gaussians in $V_c(\vec{r})$, the more diffuse are some of the Gaussians and, naturally, more time is spent in the computation of three center integrals. On the other hand, the core potential defined in terms of a very few Gaussians requires many terms in the smooth potential. Therefore, one has to find an optimum representation of the potential in the mixed space.

In Fig. 2(a), we present the band structure of Si, which is obtained from the basis set described

TABLE II. Comparison of symmetry-point energies (in eV) for Si as calculated by the ETB, OPW, and pseudopotential methods and as measured by photoemission experiments.

Energy level	ETB	OPW [a]	Pseudopotential [b] Local	Pseudopotential [b] Nonlocal	Experiment
Γ_1	−11.7	−11.7	−12.53	−12.36	−12.4 ± 0.6 [c] −12.5 ± 0.6 [d]
$\Gamma_{25'}$	0.0	0.0	0.0	0.0	
Γ_{15}	3.1	3.0	3.43	3.42	
$\Gamma_{2'}$	3.7	3.6	4.17	4.10	4.15 ± 0.05 [e]
$\Gamma_{12'}$	8.6		7.82	8.19	
$L_{2'}$	−9.5	−9.4	−10.17	−9.55	9.3 ± 0.4 [d]
L_1	−6.7	−6.7	−7.24	−6.96	−6.4 ± 0.4 [c] −6.8 ± 0.2 [d]
$L_{3'}$	−1.2	−1.1	−1.22	−1.23	−1.2 ± 0.2 [e]
L_1	2.1	1.9	2.15	2.23	
L_3	4.0	3.9	4.00	4.34	3.9 ± 0.1 [e]
$L_{2'}$	12.0	8.0			
X_1	−7.6	−7.6	−8.27	−7.69	
X_4	−2.7	−2.7	−2.99	−2.86	−2.9, [e] −2.5 ± 0.3 [d]
X_1	1.4	1.3	1.22	1.17	
$\Sigma_{1\,\min}$	4.3		−4.48	−4.47	−4.4, [e] −4.7 ± 0.3 [c,d]

[a] See Ref. 8.
[b] See Ref. 9.
[c] See Ref. 36.
[d] See Ref. 37.
[e] See Ref. 38.

above. In this model, we observe that the band order for $\Gamma_{2'}$ and Γ_{15} is in agreement with what has been concluded lately.[9] Furthermore, the indirect gap is found to be 1.2 eV, whereas the experimentally determined value is 1.14 eV. In Tables II and III, we list all the relevant energy eigenvalues and the transition energies at the symmetry points of the Brillouin zone (BZ). The same table also includes the experimental[36-40] as well as OPW[8] and pseudopotential[9] values. The agreement obtained is gratifying.

To conclude the adequacy of the basis set, we repeated similar calculations with a smaller basis set where 68 and 62 GTO's are used, and observed practically no change in the energy eigenvalues. However, the inclusion of d-type orbitals did affect the band structure. For example, the inclusion of d-type GTO's lowers the energies of $\Gamma_{25'}$ and Γ_{15} states. Therefore, the width of the valence band and the indirect gap (which is overestimated by using only s- and p-type orbitals) becomes smaller, but the intraband gap $\Gamma_{2'} - \Gamma_{15}$ becomes larger.

After this brief presentation of the Si band structure calculated by the ETB method, let us try to answer the question why a similar LCAO calculation[5] predicted reverse band order. Noting that the present calculation and the calculations of Chaney *et al.*[5] start from the same atomic charge density, one can speculate that different basis sets (Chaney *et al.*[5] used AO basis set) are responsible for different results. In order to justify this speculation, we simulated their calculation by contracting the supersecular matrix (in which each matrix element corresponds to the interaction between two GTO's) to a smaller secular matrix corresponding to the AO basis set. Formally,

TABLE III. Comparison of transition energies (in eV) for Si as calculated by the ETB, OPW, and pseudopotential methods and as measured by experiment.

Transition	ETB	OPW [a]	Pseudopotential [b] Local	Pseudopotential [b] Nonlocal	Experiment
$L_{3'} - L_1$	3.3	3.0	3.37	3.46	3.40, [c] 3.50 [d]
$\Gamma_{25'} - \Gamma_{15}$	3.1	3.0	3.43	3.42	3.45, [c] 3.41 [d]
$L_{3'} - L_3$	5.2	5.0	5.25	5.57	5.48 [c]
$X_4 - X_1$	4.9	4.9	5.28	4.83	

[a] See Ref. 8.
[b] See Ref. 9.
[c] See Ref. 39.
[d] See Ref. 40.

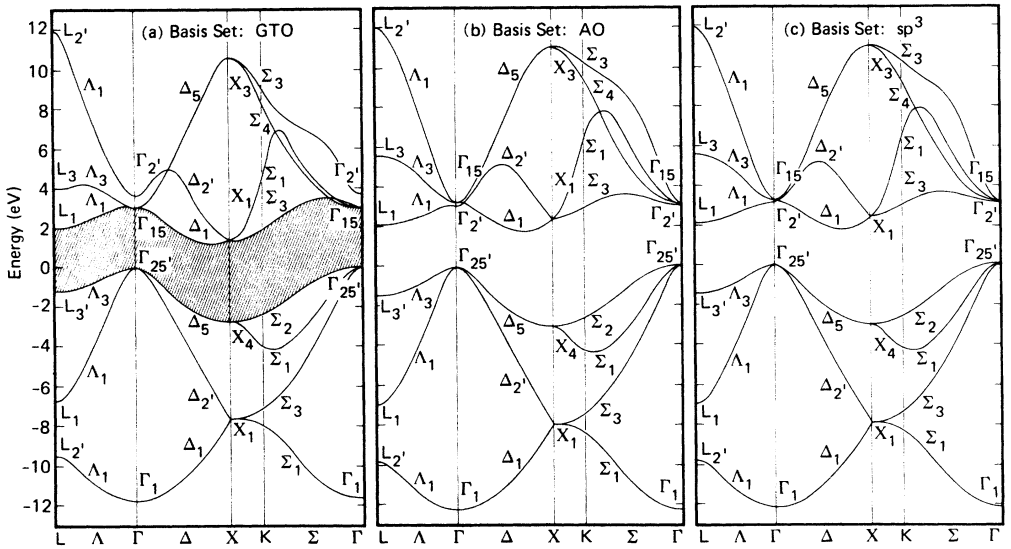

FIG. 2. Electronic band structure of silicon calculated using various basis sets in the ETB method. (a) GTO basis set, (b) AO basis set, and (c) atomic sp^3 hybrid orbital basis set. The zero of energy is taken at the edge of the valence band.

one expresses the contraction scheme, which is well known in quantum chemistry,[41] as follows:

$$\langle \phi_i | H | \phi_j \rangle = \sum_{l,m} c_{li} c_{mj} \langle G_l | H | G_m \rangle . \tag{7}$$

In this equation, c_{li} are coefficients determined from the Hartree-Fock calculations,[28] such that

$$\phi_i = \sum_l c_{li} | G_l \rangle , \tag{8}$$

where the AO, ϕ_i is constructed from the elementary GTO's, G_l. In Fig. 2(b), the band structure of silicon obtained from the basis set consisting of Si $1s$ to $3p$ atomic orbitals (i.e., by solving 18×18 secular equation) is presented. By comparing this band structure with one obtained from s- and p-type GTO's (which is not presented here) or with the one presented in Fig. 2(a), we immediately observe that most of the features of the electronic energy structure can be reproduced by the AO basis set. However, a reverse order for the lower conduction-bands at Γ is found. Therefore, we conclude that the restriction imposed on the basis set by the use of AO's is too severe for the conduction-band states of Si. The valence band is practically unchanged upon contraction from the supersecular equation to the AO secular equation, as pointed out earlier.[42] As a closing remark, we also note that GTO basis set in the ETB method enables us to do various contraction schemes. For example, sp^3 hybrid can be easily generated without redoing the computations. In Fig. 2(c), the band model of Si is generated from an sp^3-type contraction over the supersecular matrix. As one expects, the band structures in Fig. 2(b) and Fig. 2(c) are almost identical.

IV. ELECTRONIC ENERGY STRUCTURE OF β-CRISTOBALITE

For highly oxidized silicon surface, where oxygen penetrates into the lattice, the spectrum is quite similar to the UPS spectra for the amorphous SiO_2. SiO_2 is found in various crystalline and amorphous forms. The crystal structure of β-cristobalite can be visualized as an extended Si crystal where one oxygen atom is located at the middle of each Si–Si bond (or at sites of D_{3d} symmetry), and each Si atom is surrounded by four

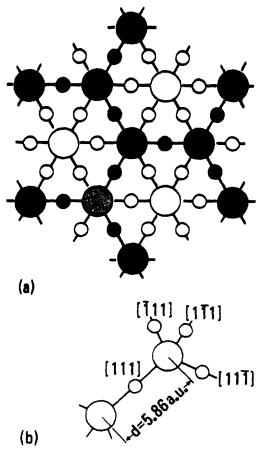

FIG. 3. Crystal structure of β-cristobalite. (a) Top view along the [111] direction. (b) Atoms in the unit cell and fundamental lattice parameters.

oxygen atoms at the tetrahedral sites. Accordingly, β-cristobalite has the O_h^7 space group. In Fig. 3, the top view along the [111] direction and the basic crystal parameters are given. For the structure of other allotropic forms of SiO_2 (where the straight Si-O-Si chain is bent, and Si-O bond distances vary), the reader may refer to Wyckoff.[43]

A. Band structure

Similar to the procedure discussed in the previous sections we carried out the band-structure calculations of β-cristobalite from the first principles. The wave functions are constructed from the linear combination of 142 s- and p-type GTO's. Here, we do not use d-type GTO's because previous calculations indicate that these are not important for the valence and lower conduction bands. The band structure is presented in Fig. 4(a), where the zero of the energy is taken at the edge of the valence band.[44] According to this band model, a 9.8-eV direct interband energy gap is obtained. The width of the valence band is found to be 10.8 eV. The photoinjection measurements[15] which are insensitive to band-edge selection rules indicated a 8.9 ± 0.2 eV band gap for amorphous SiO_2. Note that the energy-gap value of tetrahedrally coordinated solids decreases when the crystalline solid becomes amorphous. In fact, this has been justified by separate study of ours, where the amorphous SiO_2 has been simulated by bending Si-O-Si chain, and a smaller energy gap was obtained. The UPS measurements[16] (with a photon energy, $\hbar\omega = 40.8$ eV) determine the valence-band width as 11.2 eV, to be compared with our calculated value of 10.8 eV.

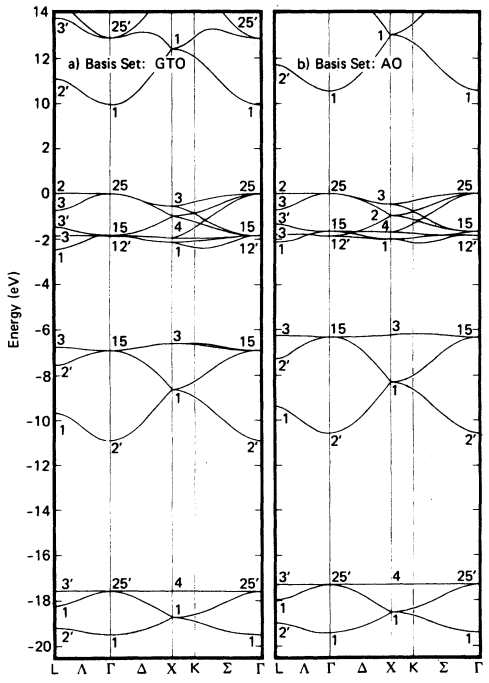

FIG. 4. Electronic band structure of β-cristobalite calculated by using the ETB method with: (a) GTO basis set, (b) AO basis set. The zero of energy is taken at the edge of the valence band.

We now discuss the orbital composition of the states at the center of the BZ. The orbital composition of an orbital i in the state $n, \vec{k}$ is defined as

$$\theta_{in}(\vec{k}) = a_{in}^2(\vec{k}) + \mathrm{Re}\left(\sum_{j(\neq i)} a_{in}^*(\vec{k}) a_{jn}(\vec{k}) W_{ij}(\vec{G}=0, \vec{k}) \right). \quad (9)$$

Here, we start with the lower-lying bands in Fig. 4(a). These bands (which are singly and triply degenerate according to the symmetry of diamond structure) are derived primarily from the s-type orbitals located at four different oxygen atoms, as pointed out by Nagel.[14] The lowest band Γ_1 (at about -20 eV) has 9%-silicon s-orbital and 20.5%-oxygen s-orbital character, and is a bonding combination of these orbitals. The triply degenerate state $\Gamma_{25'}$ (at ~ -17.5 eV) has again primarily oxygen s-orbital character with a slight mixing of silicon p-type orbitals. The XPS,[16] as well as silicon $K\beta$ and silicon $L_{2,3}$ spectral[14] measurements on amorphous SiO_2 place these lower-lying bands at -20.2 eV. The bands 7 eV above the oxygen s bands constitute the lower part of the valence band of β-cristobalite. The singlet $\Gamma_{2'}$ is the bonding combination of silicon s orbitals and oxygen p orbitals directed along the Si-O-Si chain. The triplet state Γ_{15} has similar orbital character as the singlet. Although the combination of these states varies with $\vec{k}$ wave vector, they can practically be identified as the bonding orbitals between Si and oxygen atoms as pointed out earlier by DiStefano and Eastman.[16] The predicted width, 4.5 eV, for this lower valence band seems to be about an eV smaller than the value determined by the UPS measurements.[16]

The bands at the edge of the valence band are 2.5 eV wide. They are recognized by two overlapping peaks at -1.3 and -2.4 eV in the UPS spectrum of amorphous SiO_2. The interesting feature of these bands is that the oxygen p_x, p_y, and p_z orbitals are combined to give maximum charge perpendicular to the Si-O-Si chain. Because of small overlap among these orbitals (especially along the Γ-L direction), the bands are almost dispersionless. For these reason they are called nonbonding oxygen p bands. The 5-eV energy difference[25] between the peak in silicon $K\beta$ (which corresponds to the top of the lower valence band)[14]

and the peak in oxygen $K\alpha$ (which corresponds to the top of the upper valence band)[12] is overestimated by ~1 eV in our calculations. In view of this and 1 eV difference between the calculated and measured widths of the lower valence band (as noted above), one can argue that in the amorphous structure, the widths of upper and lower valence bands increase to make the gap smaller. Note that Schneider and Fowler[25] shifted their upper valence band to consistently interpret various x-ray emission spectra.

The first conduction band is primarily derived from the Si s orbitals with a small mixing from oxygen s orbitals. The next triplet state, on the other hand, has primarily silicon p-orbital character. The shape of the lower conduction bands and their symmetries are reminiscent of silicon valence band with a smaller width due to the stretched Si-Si bond.

Regarding the conduction band, the experimental data of interest are the peaks (at 10.3, 12.0, 14.4 eV, etc.) of the optical reflectivity spectrum.[11] Similar to the interpretation made by Schneider and Fowler,[25] these peaks involve the transitions between the lower conduction and nonbonding oxygen p bands. The first peak may arise from the transition between the lowest conduction band and the second-highest valence band, i.e., $L_{2'} - L_3$. For the second peak at 12.0 eV, one may suggest the transition $L_{2'} - L_3$ (where the initial state L_3 is at the lower part of the nonbonding oxygen p band). The transition $L_1 - L_2$ (where L_1 is 1 eV above the $L_{3'}$ in the conduction band) may be responsible for the third peak.

In concluding the discussion of the energy bands, it is appropriate to comment on the previous band-structure calculations of β-cristobalite. The semiempirical work on β-cristobalite by Pantelides and Harrison[23] does not include the conduction bands. Also the lower-lying oxygen 2s bands are not included in their band model. Therefore, our comparison here is confined to the valence band. Our lower valence band is in good agreement with that obtained by Pantelides and Harrison.[23] In the upper valence band, the agreement is not too good. Contrary to their band model, we find that Γ_{15} is very close to $\Gamma_{12'}$. Furthermore, the doubly degenerate band which arises from the triplet Γ_{15} does not join X_2 to make a fourfold degenerate state at X. Our band model given in Fig. 4(a) is in good overall agreement with that reported by Schneider and Fowler.[25] The agreement becomes even better for the upper valence band when we apply the contraction from GTO basis set to the AO basis set. The band structure obtained as a result of this contraction is shown in Fig. 4(b). Note that the gap between Γ_{15} and $\Gamma_{12'}$ becomes larger here. Similar splitting (between Γ_{15} and $\Gamma_{12'}$) obtained by Schneider and Fowler[25] may well be due to the similar basis set (i.e., nonoverlapping atomiclike functions) used in their calculation. Note, however, that the AO-type basis set was shown to be inappropriate for the band structure of silicon. The comparison between Figs. 4(a) and 4(b) indicates this point once again, such that the gap between conduction and valence band is overestimated by 0.7 eV in the AO basis. The inclusion of the plane waves in the work of Schneider and Fowler[25] seems to fix the shortcomings of the AO basis set in representing the conduction band.

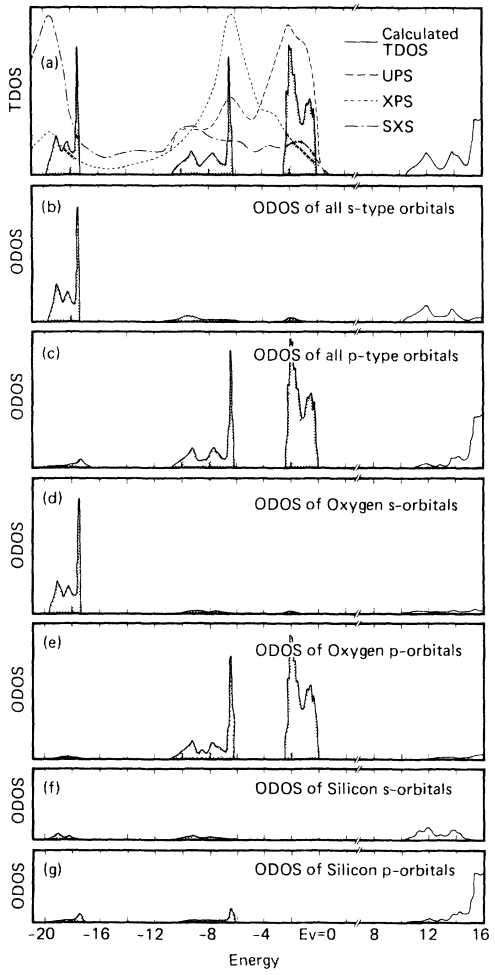

FIG. 5. State distribution analysis of β-cristobalite. (a) Total densities of states and UPS ($\hbar\omega = 40.8$ eV), XPS ($\hbar\omega = 1486$ eV), and SXS measurements for amorphous SiO_2. (b)-(g) Orbital densities of states. All the state distributions are normalized according to the total density of states. (The UPS and XPS spectra is reproduced from Ref. 16. The SXS spectra is taken from Fisher's work in Ref. 14.)

B. Total and orbital densities of states

In Fig. 5, a thorough analysis of the state distribution is presented in terms of the orbital densities of states (ODOS)[4,45,46]

$$O(E,i)=(\sigma\sqrt{2\pi})^{-1}\sum_{n,\vec{k}}\exp\{-[E_n(\vec{k})-E]^2/2\sigma^2\}\theta_{in}(\vec{k}). \tag{10}$$

This is a useful tool which projects the total densities of states into a required orbital character, or onto a particular angular direction. Therefore, it provides a systematic interpretation of the XPS, UPS data. In this study, we used the histogram technique with the Gaussian broadening $\sigma=0.1$ eV.

Figure 5(a) shows our calculated total density of states (TDOS) for β-cristobalite. In the same panel we reproduce the UPS, XPS, and soft-x-ray (SXS) intensities.[16] At this point we would like to point out that caution should be exercised in comparing spectra of amorphous SiO_2 with the state distribution of perfect crystalline SiO_2. As pointed out earlier, the interband energy gap decreases because of the broadening of the band edges. To compare the major peaks of the experimental spectra with our total density of states, we aligned the Fermi levels. In Fig. 5(a), the energy positions of two overlapping peaks, in the 40.8 eV photon energy, UPS spectra,[16] lie on the two major peaks of our total densities of states. These two peaks, which are not resolved by Ibach and Rowe,[17] are characteristic features of the oxidized silicon surfaces.[18] At the lower part of the valence band, the peak and the lower shoulder at ~ -10 eV line up with the two peaks of bonding oxygen p bands. For the lower-lying oxygen s band, the SXS spectra resolves one peak, though our density of states shows two additional peaks arising from the states at the L-symmetry point of the BZ. Although fine structures at the upper portion of the valence band are not resolved in the experimental spectra, the overall agreement is good. This suggests that in SiO_2 the local order of the atoms plays primary role in determining the general features of the state distribution.

In Figs. 5(b)–5(g) the orbital analyses of the state distribution are shown. The distribution in Fig. 5(b), clearly indicates that the lower lying bands below the valence band and the lower conduction band are derived from the s-type orbitals, as pointed out before. Figure 5(c) projects the p-type orbital character of the total densities of states and shows that the valence-band and upper-conduction-band states of SiO_2 have p-orbital character. To find the atomic origins of the states, we examine the rest of the panels. Figure 5(d) indicates that the narrow lower-lying bands at -20 eV are primarily derived from the oxygen s orbitals, whereas Fig. 5(e) shows that the oxygen p orbitals are responsible for the distribution of the valence band. Finally, in Figs. 5(f) and 5(g), we do the same projection for silicon s and p orbitals, and show that silicon s and p orbitals appear primarily in the conduction band.

C. Static effective charge

Having seen the orbital contribution and the orbital densities of states, one can go one step further and define the total electronic occupancy of an atom in the unit cell. This can be achieved by summing over the orbitals (GTO or AO) located at a given atom t.

$$\xi_t=\frac{1}{N}\sum_{i\in t}\sum_{n,\vec{k}}^{\text{occ}}\theta_{in}(\vec{k}). \tag{11}$$

In Eq. 11, the number of points sampled in the BZ, which is denoted by N, is needed to normalize the occupancy. At this point, it would be appropriate to discuss the static effective charge.[23] Ambiguities in associating effective charges with ions arise from the fact that there is no absolute way of dividing the charge among the ions in the unit cell. The bond charge in tetrahedrally coordinated semiconductors makes the definition of the static effective charge even more difficult. Here, we use the definition of the total occupancy and try to determine the net charge on an atom t by using the following expression:

$$Z_t^*=\xi_t-Z_t, \tag{12}$$

where Z_t is the nuclear charge of the free atom. Using Eq. (11), our calculation yields 1.5 electrons for the net charge on oxygen in β-cristobalite. In the context of the bond-orbital model, Pantelides and Harrison calculated the static effective charge of β-cristobalite and found 1.3 extra electrons on oxygen.

Realizing the ambiguity in relating the static effective charge to the crystal potential, in the present work we use the overlapping atomic potentials rather than the ionic potentials. Certainly, the self-consistent solution of the problem would wipe out all the uncertainties in the choice of the potential, but the overlapping atomic potential as used in the present work is known[8] to be a good approximation.

D. State charge density

To appreciate bonding in SiO_2 in a pictorial fashion, we calculate the charge densities of the states along Si-O-Si chain. The results[47] are shown in Figs. 6 and 7. Figure 6, presents the charge density of several states at the center of the BZ. In

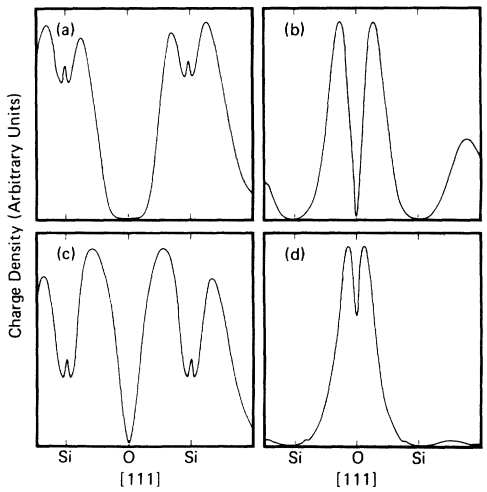

FIG. 6. Charge distribution of various states at the center of the zone. (a) First conduction-band state, (b) first valence-band state, (c) lowest bonding oxygen p state, (d) lowest bonding oxygen s band state. (Arbitrary units for the charge density.)

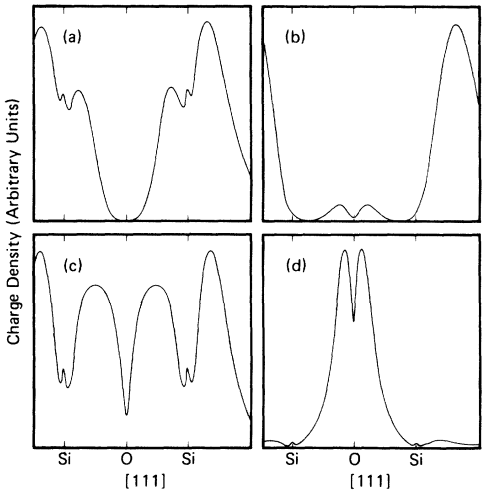

FIG. 7. Charge distribution of various states at the Baldereshi point, $\vec{k}^* = (2\pi/a)(0.622, 0.245, 0)$. The order of the states is the same as in Fig. 6.

Fig. 6(a), the charge distribution of the state at the edge of the conduction band Γ_1 clearly indicates that this state derives from the silicon s orbitals. In Fig. 6(b), the charge distribution of the state at the edge of the valence band, Γ_{25} shows a considerable p-orbital component along the chain. In general, for these nonbonding oxygen bands, p orbitals are directed perpendicular to the chain. In Fig. 6(c), the charge density of the state $\Gamma_{2'}$ in lower valence band illustrates the bonding combination between Si s and oxygen p orbitals along Si-O-Si chain. Finally, the charge density of the lower-lying oxygen s bands Γ_1 are plotted in Fig. 6(d). In Fig. 7 similar charge distributions are shown at the Baldereshi point[48] where the state charge distribution is similar to the total charge distribution.

V. PARAMETRIZATION OF THE ETB HAMILTONIAN

In ETB, as well as in other methods of band-structure calculation, the fact is that the computational effort increases with the increasing number of atoms in the unit cell. Study of larger systems, such as amorphous SiO_2 or other allotropic forms of SiO_2 (where the number of SiO_2 molecules is generally larger than two), then becomes rather unpractical. Therefore, a simple, yet realistic method of calculations becomes desirable. A need for a simplified method is even greater for the study of the reconstructed surfaces, where the superlattice formation makes the surface unit cell much bigger than the unit cell of the ideal surface. A good example of this is the 7×7 reconstruction of the Si(111) surface. With a simplified method one can, at least, calculate the spectrum for various geometries and compare it with experiment. In this spirit, Ciraci and Batra[49] attempted to determine the reconstruction geometry of cleaved Si(111) surface. The extended Hückel method[50] is one of the parametrized versions of the tight-binding method, where the Hamiltonian matrix elements are determined from chemical intuition using the empirical expression,

$$H_{ij} = \tfrac{1}{2}K(\epsilon_i + \epsilon_j)S_{ij}, \tag{13}$$

where ϵ_i and ϵ_j are usually taken as the ionization energies of the orbitals. K is an empirical constant. Determining the energy parameters from Eq. (13) without any computational effort makes the extended Hückel method most appealing. In

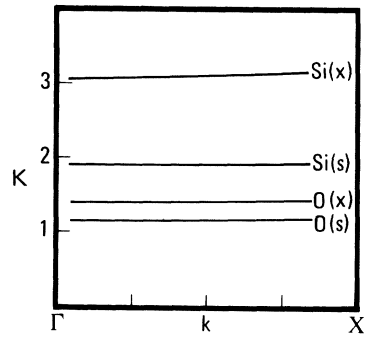

FIG. 8. Parameters K [Eq. (13)] versus wave vector of β-cristobalite. Si(x), Si(s), O(x), etc., denote the diagonal matrix elements for atomic valence orbitals.

this section, we attempt to test the validity of Eq. (13) by using our Hamiltonian and overlap matrices calculated for β-cristobalite. Our objective is to explore the following points: (i) Can one choose one single empirical parameter K? (ii) Is this parameter dispersionless?

In order to answer these questions, we parametrized the ETB Hamiltonian according to the relation given by Eq. (13). In Fig. 8 we present the values of K along the Γ-X direction. By examining this figure and the results for other symmetry directions, one reaches the following conclusion. The value of K depends on the type of orbital, but it is a real quantity. Therefore, the use of a single K for entire Hamiltonian matrix may not be appropriate. Furthermore, K is practically dispersionless. In view of these conclusions, we propose the following parametrization scheme:

$$H_{ij}(\vec{k}) = I_{ij} S_{ij}(\vec{k}), \tag{14}$$

where I_{ij} are to be determined from the ETB secular equation for a "smaller" system. According to this equation, the wave vector and the geometry dependence of H_{ij} is then determined from the overlap matrix element $S_{ij}(\vec{k})$. The latter, however, can be calculated easily for different geometries and $\vec{k}$ vectors.

VI. CONCLUSIONS

We have shown that the ETB method can be successfully used for investigating band structure of solids from first principles. The choice of the basis set is an important aspect because for an inappropriate choice one may end up with improper ordering of bands, as we found for silicon. The implementation of the contraction scheme from quantum chemistry into the ETB method makes it a very flexible tool in the studies of the electronic structure.

Our results for β-cristobalite have revealed that the state distributions of regular and amorphous SiO_2 have similar features. However, the widths of nonbonding and bonding oxygen p bands increase due to the increasing overlaps in distorted tetrahedra of amorphous SiO_2. Bonds in SiO_2 develop between the bonding combination of silicon s, p, and oxygen p orbitals along the Si-O-Si chain.

We acknowledge helpful discussions with Dr. P. S. Bagus, Dr. F. Herman, and Dr. W. E. Rudge.

---

*Present Address: Turkiye Bilimselve Teknik Arastirma Kurumu Marmara Scientific and Industrial Research Institute, Gebze-Kocaeli, Turkey.

[1]E. E. Lafon and C. C. Lin, Phys. Rev. 152, 579 (1966); R. C. Chaney, T. K. Tung, C. C. Lin, and E. E. Lafon, J. Chem. Phys. 52, 361 (1970).

[2]J. C. Callaway and J. L. Fry, *Computational Methods in Band Theory* (Plenum, New York, 1974), p. 512; J. Callaway and C. S. Wang, Phys. Rev. B7, 1096 (1973).

[3]J. E. Simmons, C. C. Lin, D. F. Fouquet, E. E. Lafon, and R. C. Chaney, J. Phys. C 8, 1549 (1975).

[4]S. Ciraci and I. P. Batra, Phys. Rev. B 15, 3254 (1977); I. P. Batra and S. Ciraci, Bull. Am. Phys. Soc. 21, 7 (1976); S. Ciraci and I. P. Batra, *ibid.* 21, 322 (1976).

[5]R. C. Chaney, C. C. Lin, and E. E. Lafon, Phys. Rev. B 3, 459 (1971).

[6]D. J. Stukel and R. N. Euwema, Phys. Rev. B 4, 1635 (1970).

[7]D. E. Aspnes and A. A. Studna, Solid State Commun. 11, 1375 (1972).

[8]F. Herman, R. L. Kortum, C. D. Kuglin, and J. P. Van Dyke, *Methods in Computational Physics* (Academic, New York, 1968), Vol. 8, p. 193.

[9]J. Chelikowsky and M. L. Cohen, Phys. Rev. B 10, 5095 (1974).

[10]H. R. Philipp, Solid State Commun. 4, 73 (1966).

[11]H. R. Philipp, J. Phys. Chem. Solids 32, 1935 (1971).

[12]G. Klein and H-U Chun, Phys. Status Solidi B 49, 167 (1962).

[13]A. O. Ershov, D. A. Goganov, and A. P. Lukirskii, Fiz. Tverd. Tela 7, 2355 (1965) [Sov. Phys.-Solid State 7, 1903 (1966)].

[14]G. Wiech, *Soft X-Ray Band Spectra*, edited by D. J. Fabian (Academic, New York, 1968); D. W. Fisher, J. Chem. Phys. 42, 3814 (1965); *Advances in X-Ray Analysis*, edited by B. L. Henke, J. B. Newkirk, and G. R. Mallett (Plenum, New York, 1970), Vol. 13, p. 159; D. J. Nagel, in *Advances in X-Ray Analysis*, edited by B. L. Henke, J. B. Kewkirk, and G. R. Mallett (Plenum, New York, 1970), Vol. 13, p. 182.

[15]T. H. DiStefano and D. E. Eastman, Solid State Commun. 9, 2259 (1971).

[16]T. H. DiStefano and D. E. Eastman, Phys. Rev. Lett. 25, 1560 (1971).

[17]H. Ibach and J. E. Rowe, Phys. Rev. B 10, 710 (1974).

[18]L. F. Wagner and W. E. Spicer, Phys. Rev. B 4, 1512 (1974).

[19]H. Ibach, K. Horn, D. Dorn, and H. Lüth, Surf. Sci. 38, 433 (1973); and H. Ibach (private communication).

[20]A. J. Bennett and L. M. Roth, J. Phys. Chem. Solids 32, 1951 (1971).

[21]K. L. Yip and W. B. Fowler, Phys. Rev. B 10, 1400 (1974).

[22]S. T. Pantelides and W. A. Harrison, Phys. Rev. B 13, 2667 (1976); S. T. Pantelides, Phys. Lett. A 54, 401 (1975).

[23]W. A. Harrison, Phys. Rev. B 8, 4487 (1973); W. A. Harrison and S. Ciraci, *ibid.* 10, 1516 (1974).

[24]M. A. Reilly, J. Phys. Chem. Solids 31, 1041 (1970).

[25]P. M. Schneider and W. B. Fowler, Phys. Rev. Lett. 36, 425 (1976).

[26]F. Bloch, Z. Phys. 52, 555 (1928).

[27]J. C. Slater and G. F. Koster, Phys. Rev. 94, 1498 (1954).

[28]In order to start with the accurate charge densities of atoms, we have used Hartree-Fock wave functions. For details see C. Roetti and E. Clementi, J. Chem. Phys. 45, 350 (1965).
[29]R. H. Parmenter, Phys. Rev. 86, 552 (1952); J. L. Fry (private communication).
[30]Private communications with Dr. W. E. Rudge, Dr. I. B. Ortenburger, and Dr. F. Herman.
[31]R. N. Euwema and D. J. Stukel, Phys. Rev. B 12, 4692 (1970).
[32]Note that the charge density obtained from the overlapping atomic charge densities fails to account accurately the x-ray form factors of covalent solids.
[33]T. Ahlenius, J-L Calais, and P-O Löwdin, J. Phys. C 6, 1896 (1973).
[34]S. Ciraci, J. Phys. Chem. Solids 36, 557 (1975).
[35]We have used GTO's determined by S. Huzinaga. For details see S. Huzinaga, J. Chem. Phys. 42, 1293 (1965).
[36]L. Ley, S. Kowalcyzk, R. Pollak, and D. A. Shirley, Phys. Rev. Lett. 29, 1088 (1972).
[37]W. D. Grobman and D. E. Eastman, Phys. Rev. Lett. 29, 1508 (1972).
[38]W. E. Spicer and R. C. Eden, in *Proceedings of the Ninth International Conference of the Physics of Semiconductors, Moscow, 1968* (Nauka, Leningrad, 1968), Vol. 1, p. 61.
[39]R. R. L. Zucca, J. P. Walter, Y. R. Shen, and M. L. Cohen, Solid State Commun. 8, 627 (1970).
[40]M. Welkowsky and R. Braunstein, Phys. Rev. B 5, 497 (1972).
[41]For the contraction scheme see, for example, E. Clementi, *Proceedings of the International Symposium on Selected Topics in Molecular Physics* (Verlag Chemie, Ludwigsburg, Germany, 1970), p. 199.
[42]S. Ciraci, Phys. Status Solidi B 70, 689 (1975).
[43]R. W. G. Wyckoff, *Crystal Structures* (Interscience, New York, 1963), Vol. I, p. 312.
[44]In order to be confident about the convergence of the band structure, we repeated the calculations for (i) different basis sets, (ii) different representation of the crystal potential in mixed space, and (iii) different number of neighboring atoms included in the calculations. The results presented in Sec. IV correspond to converged band structure for all three possibilities.
[45]J. Friedel, Adv. Phys. 3, 446 (1954).
[46]R. S. Mulliken, J. Chem. Phys. 23, 1833 (1955); T. B. Grimley, J. Phys. C 3, 1934 (1970); D. J. M. Fassaert and A. Van Der Avoird, Surf. Sci. 55, 291 (1976); I. P. Batra and C. R. Brundle, *ibid.* 57, 12 (1976).
[47]For the sake of computational convenience, the state charge densities presented in Figs. 6 and 7 are normalized for each state. Therefore, one should not compare the densities in different panels.
[48]A. Baldereshi, Phys. Rev. B 7, 5212 (1970).
[49]S. Ciraci and I. P. Batra, Solid State Commun. 18, 1149 (1976).
[50]R. Hoffman, J. Chem. Phys. 39, 1397 (1963).

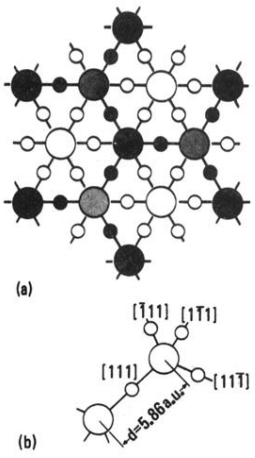

FIG. 3. Crystal structure of β-cristobalite. (a) Top view along the [111] direction. (b) Atoms in the unit cell and fundamental lattice parameters.

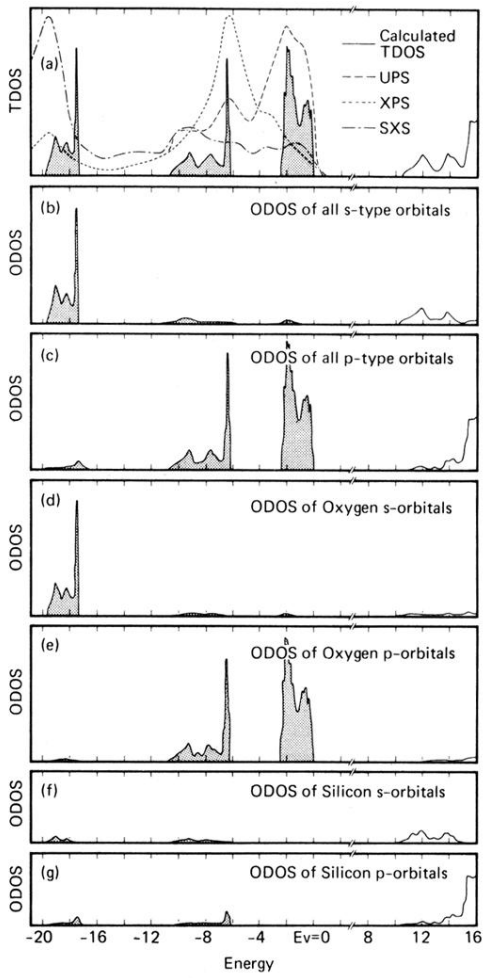

FIG. 5. State distribution analysis of β-cristobalite. (a) Total densities of states and UPS ($\hbar\omega = 40.8$ eV), XPS ($\hbar\omega = 1486$ eV), and SXS measurements for amorphous SiO_2. (b)–(g) Orbital densities of states. All the state distributions are normalized according to the total density of states. (The UPS and XPS spectra is reproduced from Ref. 16. The SXS spectra is taken from Fisher's work in Ref. 14.)